Lehrstuhl für Bildverarbeitung
Institute of Imaging & Computer Vision

Wavelet Based Denoising by Correlation Analysis for High Dynamic Range Imaging

Jens N. Kaftan and André A. Bell and Claude Seiler and Til Aach
Institute of Imaging and Computer Vision
RWTH Aachen University, 52056 Aachen, Germany
tel: +49 241 80 27860, fax: +49 241 80 22200
web: www.lfb.rwth-aachen.de

in: IEEE International Conference on Image Processing (ICIP2009). See also BIBTEX entry below.

BIBTEX:

```
@inproceedings{KAF09b,
author = {Jens N. Kaftan and Andr{\'e} A. Bell and Claude Seiler and Til Aach},
title = {Wavelet Based Denoising by Correlation Analysis for High Dynamic Range Imaging},
booktitle = {IEEE International Conference on Image Processing (ICIP2009)},
publisher = {IEEE},
address = {Cairo},
month = {November 7-11},
year = {2009},
pages = {3857--3860}}
```

© 2009 IEEE. Personal use of this material is permitted. However, permission to reprint/republish this material for advertising or promotional purposes or for creating new collective works for resale or redistribution to servers or lists, or to reuse any copyrighted component of this work in other works must be obtained from the IEEE.

document created on: January 5, 2010
created from file: hdr-correlation-denoising.tex
cover page automatically created with CoverPage.sty
(available at your favourite CTAN mirror)

RWTH AACHEN
RHEINISCH-WESTFÄLISCHE TECHNISCHE HOCHSCHULE AACHEN

WAVELET BASED DENOISING BY CORRELATION ANALYSIS FOR HIGH DYNAMIC RANGE IMAGING

Jens N. Kaftan, André A. Bell, Claude Seiler, Til Aach

Institute of Imaging and Computer Vision, RWTH Aachen University, Germany

ABSTRACT

High dynamic range (HDR) imaging is used to acquire the full dynamic range of a scene with a camera of limited dynamic range. To this end, an exposure set of the scene is acquired, followed by the linearization of each image with the inverse camera transfer function (CTF), which needs to be measured or estimated. Subsequently, the images are combined into one HDR image. Several weighting functions have been proposed for this combination. Naturally, each individual image is afflicted with noise from the acquisition process. The resulting HDR image features a higher SNR than the acquired images as a consequence of the weighted averaging during reconstruction. We show that the fact that the individual images partially show the same structures with independent noise can be utilized to further improve the SNR. Thus, we propose a wavelet-based denoising using correlation analysis between different images from the exposure set that outperforms the denoising properties of commonly applied weighted averages.

Index Terms— High dynamic range imaging, Noise, Noise reduction, Correlation, Image enhancement

1. INTRODUCTION

The dynamic range of natural scenes often exceeds the dynamic range of a conventional digital camera. Therefore, single images exhibit underexposed and overexposed areas. To overcome this limitation, several methods have been developed that combine differently exposed images of the same scene into one high dynamic range (HDR) image. This HDR image has a greater dynamic extent than each individual low dynamic range (LDR) image.

The HDR imaging process requires the knowledge of the mostly nonlinear camera transfer function (CTF) of the camera. This CTF can be measured using, e.g., charts [1] or radiometric methods [2], while proposed estimation methods include model-based fitting using, e.g., a gamma curve or other parametric functions [3, 4, 5]. Furthermore, general polynomials [6] as well as constrained piecewise linear functions [7] or a smoothness constraint [8] have been applied to estimate the CTF.

After measuring or estimating the CTF, the LDR images of the exposure set are linearized with the inverse of the CTF, aligned in range, and combined into one HDR image. Naturally, each individual image of the exposure set contains noise. This noise is reduced by the weighted averaging operation applied to combine the exposure set into the HDR image. In the literature several weighting functions have been proposed for this combination. Mann proposed the derivative of the CTF as weighting function w_{Mann} [3]. This idea is based on the observation that the output of the sensor is most reliable in areas of highest slope of the CTF and least reliable in areas where the slope of the CTF is lowest. A triangular function w_{Debevec}, which weights pixel values near the black and white levels as unreliable and gray values in between as most reliable, has been proposed by Debevec [8]. Mitsunaga proposed a weighting function $w_{\text{Mitsunaga}}$ that is based on the estimated signal to noise ratio (SNR) [6]. All these weighting functions have been compared to the plain average w_{Mean} in [9]. Of course one can only expect an SNR increase in case of partial range overlap between different images of the exposure set, i.e., if parts of the scene are observable in more than one image. It has been discussed how to reduce the acquisition time of the HDR imaging by minimizing this range overlap [10]. This leads to a trade-off between the exposure set size and the SNR in HDR imaging [11].

In case of a partial overlap of the images in the range domain, the exposure set contains sets of two or more images showing identical parts of the scene under different exposure settings. These areas exhibit the same structural information, but independent noise. Instead of only combining these areas by a weighted average, we show that a higher SNR_{gain} can be achieved. To this end, we identify structures in the image by a correlation analysis. The noise is then reduced by a wavelet-based denoising method using the correlation analysis result to control the noise reduction degree locally. We show that the achieved SNR_{gain} surpasses the SNR_{gain} achieved in conventional HDR imaging.

2. ALGORITHM DESCRIPTION

Noise reduction methods have to be edge preserving, i.e., the structural information in the image shall not be affected. Several methods to achieve this are known, which are designed to lower the noise energy and simultaneously not smooth across edges, e.g., bilateral filtering [12] and nonlinear dif-

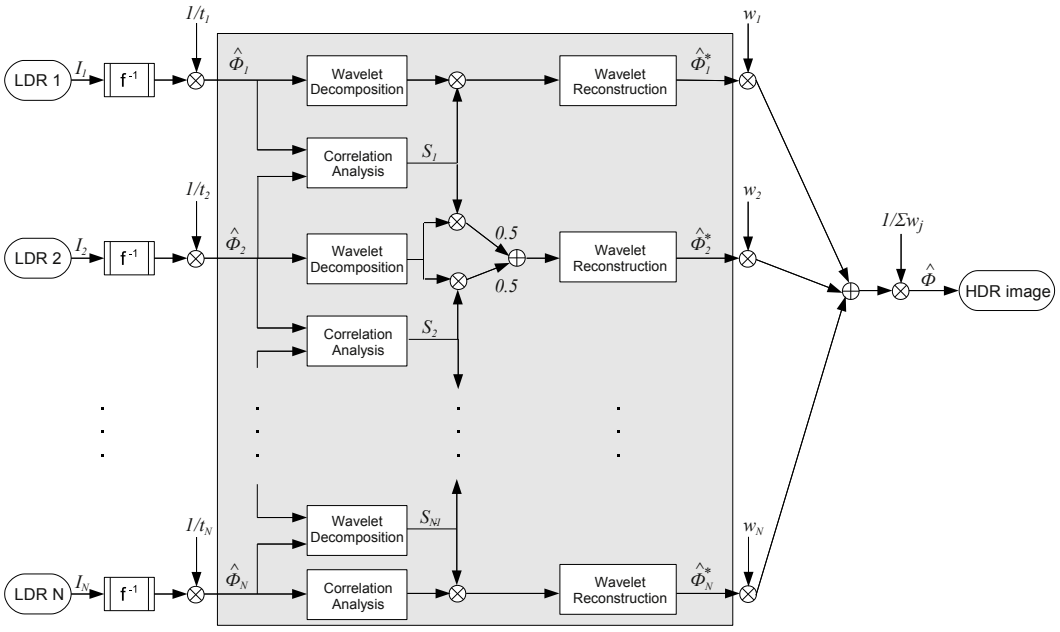

Fig. 1. Diagram showing the wavelet-based denoising using correlation analysis and its integration into HDR imaging. All LDR images $I_j, j \in 1, \ldots, N$, of the exposure set are linearized with respect to the CTF and afterwards aligned in the range domain $(1/t_j)$. In conventional HDR imaging, these images are weighted and averaged into one HDR image, while skipping the steps inside the gray block. This area highlights the steps and methods of the proposed wavelet-based denoising approach. All images $\hat{\phi}_j$ are wavelet transformed. The correlation analysis is calculated on pairs of images of adjacent exposure times and the resulting similarity images are denoted by $S_i = S_{m,n}(\hat{\phi}_i, \hat{\phi}_{i+1}), i \in 1, \ldots, N-1$. Afterwards the correlation analysis result is utilized for the wavelet domain denoising and followed by an inverse wavelet transform. The resulting noise reduced images $\hat{\phi}_j^*$ are then combined as in conventional HDR imaging.

fusion [13]. Wavelet-based denoising techniques utilize the fact that white noise is invariant under orthogonal transformation. Structure, hence, is represented by few dominant coefficients while white noise is spread across a range of small coefficients [14]. Conventional noise reduction in the wavelet domain is based on erasing small coefficients that fall below a threshold. By using correlation analysis between two images with the same structures but independent noise the difficulty of selecting a suitable threshold can be omitted [15]. This method has furthermore been successfully applied to computed tomography (CT) scans [16].

Fig. 1 shows an overview of our algorithm and how we combine the wavelet-based noise reduction, correlation analysis, and high dynamic range imaging. Light $E^*(x, y)$ (irradiance) incident on the imaging sensor is integrated over the area A of each sensor element and results in an amount of radiant power $\phi_{m,n}$ for a pixel at position m, n

$$\phi_{m,n} = \iint_{x=m,y=n}^{m+\Delta x,n+\Delta y} E^*(x, y)\, dA \tag{1}$$

yielding the radiant energy $Q_{j,m,n} = t_j \cdot \phi_{m,n}$ collected in the sensor element during the exposure time t_j with $j \in 1, \ldots, N$ being the index of the exposure time in an exposure set. Next, the nonlinear behavior of the imaging system, e.g., the nonlinear sensor sensitivity near the noise floor and the full well capacity, or nonlinearities in the electronics, change the sensor response. These nonlinearities are reflected in the CTF f. In the presence of noise n_Q, e.g., thermal noise, read-out noise, or quantum noise, before the CTF and additional noise n_f, e.g., quantization noise, after the CTF, the resulting output I_j is given by (cf., [3])

$$I_{j,m,n} = f(Q_{j,m,n} + n_Q) + n_f \tag{2}$$

Without fixed pattern noise (FPN), which is accounted for by flat field correction, the major noise influences n_Q can be modeled as Gaussian noise [17]. We intend to calculate an estimate $\hat{\phi}_{m,n}$ of the HDR image $\phi_{m,n}$. To this end, the partial estimates $\hat{\phi}_{j,m,n}$ from each individual low dynamic range image, given by

$$\hat{\phi}_{j,m,n} = \frac{1}{t_j} f^{-1}(I_{j,m,n}) \tag{3}$$

are combined by the weighted average

$$\hat{\phi}_{m,n} = \frac{\sum w(\hat{\phi}_{j,m,n}, I_{j,m,n})\hat{\phi}_{j,m,n}}{\sum w(\hat{\phi}_{j,m,n}, I_{j,m,n})} \quad (4)$$

with w being a weighting function that represents the reliability of the individual estimates $\hat{\phi}_{j,m,n}$.

To now integrate the noise reduction scheme into this framework, we calculate the wavelet decomposition of each estimate $\hat{\phi}_{j,m,n}$ up to decomposition level L. Furthermore, we calculate a similarity image S^l for the individual scales $l = 1, \ldots, L$ of the wavelet decomposition. Let $W_A^l(a)$ denote the lowpass approximation image of the wavelet decomposition of an image a at level l. The similarity measure can then be defined as the correlation coefficient given by

$$S^l_{m,n}(\hat{\phi}_j, \hat{\phi}_{j+1}) = \frac{\mathrm{Cov}_{m,n}\Big(W_A^{l-1}(\hat{\phi}_j), W_A^{l-1}(\hat{\phi}_{j+1})\Big)}{\sqrt{\mathrm{Var}_{m,n}\Big(W_A^{l-1}(\hat{\phi}_j)\Big)\mathrm{Var}_{m,n}\Big(W_A^{l-1}(\hat{\phi}_{j+1})\Big)}} \quad (5)$$

with covariance

$$\mathrm{Cov}_{m,n}(a,b) = \frac{1}{|\Omega_{m,n}|}\sum_{x\in\Omega_{m,n}}\Big(a(x)-\bar{a}\Big)\Big(b(x)-\bar{b}\Big) \quad (6)$$

and variance

$$\mathrm{Var}_{m,n}(a) = \frac{1}{|\Omega_{m,n}|}\sum_{x\in\Omega_{m,n}}\Big(a(x)-\bar{a}\Big)^2 \quad (7)$$

calculated over some neighborhood $\Omega_{m,n}$ of $|\Omega_{m,n}|$ elements around pixel position m, n. The average value within this neighborhood of some image a is denoted by $\bar{a}$. Due to the scale structure of the wavelet decomposition, the correlation analysis is based on a scale dependent amount of pixels for a fixed size neighborhood $\Omega_{m,n}$. The resulting similarity images S^l contain values in the range $[-1; 1]$. Values near 1 represent high correlation, while values near 0 represent no correlation. Negative values towards -1 would indicate anti-correlation, which we will not observe in the image pairs from the exposure set.

Let $W_H^l(a)$, $W_V^l(a)$, and $W_D^l(a)$, denote the horizontal, vertical and diagonal detail images of the wavelet decomposition of an image a at level l, respectively. The result of the correlation analysis, i.e., the calculated similarity values are now point-wise multiplied with the detail coefficients, according to

$$W^{*l}_{\{H,V,D\},m,n} = W^l_{\{H,V,D\},m,n}\left(S^l_{m,n}(a,b)\right)^p \quad (8)$$

The strength of the noise reduction can be steered by the power coefficient p (cf., [16]). After inverse wavelet transform of the weighted coefficients, the HDR image is calculated as usual using Eq. (4) with the noise reduced versions $\hat{\phi}^*_j$ of the initial input estimates $\hat{\phi}_j$.

3. EXPERIMENTAL SETUP

To evaluate the SNR improvement of the presented algorithm, we have generated a simulated high dynamic range scene containing objects of varying contrast to the background and varying size (see Fig. 2). Due to the experimental setup we constrain the scene to be perfectly still at this point, which otherwise might cause ghosting artifacts in the reconstructed HDR image. Next, we have virtually acquired low dynamic range images with $k = 8$ different exposures and several linear and nonlinear CTFs (see [9]) using an additive Gaussian noise model with a SNR of 15dB, 20dB, and 30dB, respectively. For each of the described weighting functions w_{Mann}, w_{Debevec}, $w_{\text{Mitsunaga}}$, and w_{Mean} we have calculated the achieved SNR_{gain} as compared to the input SNR. We have repeated all of these settings 100 times and calculated the mean SNR_{gain} and its variance. The LDR images were generated to show the same structure of the scene in $3-4$ out of 8 images. The expected SNR_{gain} for the conventional HDR imaging would therefore be $\text{SNR}_{\text{gain}} = 10\log_{10}4 \approx 6\text{dB}$.

Furthermore we have repeated all those experiments under all different settings from above, this time including the wavelet-based denoising by correlation analysis. We have varied the wavelet function among the Daubechies wavelets db1 and db2 both under varying maximum decomposition depth $L \in \{1, 2, 3\}$ and $p \in \{1, 2, 4\}$. For these additional settings we have once again repeated the experiments 100 times and calculated the improved mean $\text{SNR}^*_{\text{gain}}$ and its variance relative to the SNR_{gain} of conventional HDR imaging.

4. RESULTS AND CONCLUSION

Conventional HDR imaging achieved an SNR_{gain} of $2.5\text{dB} - 6\text{dB}$. These experimental results are slightly lower than the expected SNR_{gain}, but still a good match. For the Daubechies wavelet db1, $p = 1$, and $L = 1$, i.e., wavelet denoising on the first detail level only, the presented denoising algorithm already achieved an *additional* $\text{SNR}^*_{\text{gain}}$ of $2.1\text{dB} - 3.0\text{dB}$. With $L = 2$ this increases to $2.9\text{dB} - 5.2\text{dB}$. At detail level $L = 3$ the SNR increased by $3.1\text{dB} - 5.5\text{dB}$ compared to conventional HDR imaging. Increasing p to 4 with $L = 3$, we achieved an $\text{SNR}^*_{\text{gain}}$ of $5.5\text{dB} - 8.7\text{dB}$. Switching to Daubechies wavelet db2 further increases the $\text{SNR}^*_{\text{gain}}$ by 2dB on average. Note, however, that the neighborhood $\Omega_{m,n}$ of the correlation analysis is dependent on the support region of the chosen wavelet and hence the region around edges where high correlations are obtained expands. As, at the same time, the wavelet coefficient shrinkage is reduced in such regions, longer reaching wavelets result in lower noise removal near the edges. Fig. 2 shows an example of the achieved noise reduction.

In this paper we have introduced a wavelet-based denoising by correlation analysis for HDR imaging. We have experimentally shown that higher noise reduction as in conven-

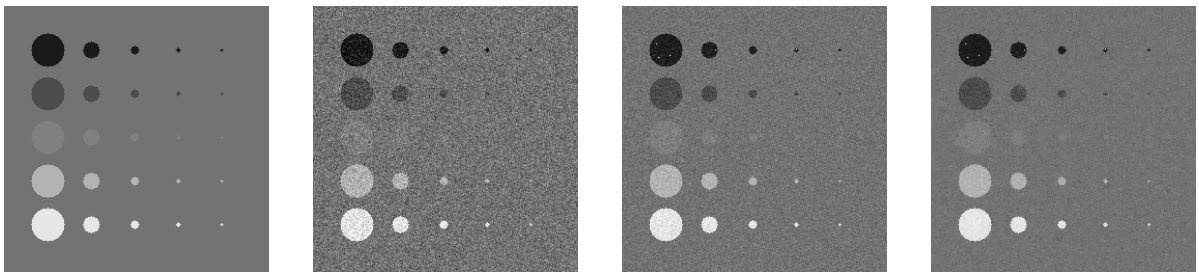

(a) (b) (c) (d)

Fig. 2. Example images of our experiments. Image (a) shows the HDR scene and image (b) the same scene with added Gaussian noise of SNR $= 15$dB. Figures (c) and (d) show the reconstructed images with standard HDR imaging (mean weighting) and wavelet based denoising (p=2, L=3, db1, mean weighting), respectively. The SNR_{gain} in (c) is 6dB and 10dB in (d).

tional HDR imaging can be achieved, while at the same time structures are preserved. To this end, we have utilized that neighboring exposures from the ordered exposure set show the same structure in different exposure, but with independent noise. Therefore, the structure could be straightforwardly identified by a correlation analysis resulting in an improved noise reduction for HDR imaging.

In the future we plan to extend our experiments to images that include Poisson-distributed noise, which could be accounted for using, e.g., Anscombe's variance stabilization transformation as described in [14], and proceed as if the data arose from the Gaussian noise model. Addressing ghosting-artifacts arising from not perfectly still scenes, however, is in itself a challenging topic. We believe that algorithms to detect and remove ghosting-artifacts in conventional HDR can be mostly adjusted and integrated into our framework.

5. REFERENCES

[1] Y. C. Chang and J. F. Reid, "RGB Calibration for Color Image Analysis in Machine Vision," *IEEE Transactions on Image Processing*, vol. 5, no. 10, pp. 1414–1422, 1996.

[2] A. A. Bell, J. N. Kaftan, D. Meyer-Ebrecht, and T. Aach, "An Evaluation Framework for the Accuracy of Camera Transfer Functions Estimated from Differently Exposed Images," in *7th Southwest Symposium on Image Analysis and Interpretation, SSIAI 2006*, 2006, pp. 168–172.

[3] S. Mann, "Comparametric equations with practical applications in quantigraphic image processing," *IEEE Transactions on Image Processing*, vol. 9, no. 8, pp. 1389–1406, 2000.

[4] Y. Tsin, V. Ramesh, and T. Kanade, "Statistical calibration of CCD imaging process," in *IEEE International Conference on Computer Vision. ICCV 2001*, 2001, vol. 1, pp. 480–487.

[5] D. Hasler and S. Süsstrunk, "Modeling the Opto-Electronic Conversion Function (OECF) for Application in the Stitching of Panoramic Images," in *International Conference on Imaging Systems (ICIS)*, 2002, pp. 379–380.

[6] T. Mitsunaga and S. K. Nayar, "Radiometric self calibration," in *IEEE Conference on Computer Vision and Pattern Recognition. CVPR 1999*, 1999, vol. 1, pp. 374–380.

[7] F. M. Candocia and D. A. Mandarino, "A semiparametric model for accurate camera response function modeling and exposure estimation from comparametric data," *IEEE Transactions on Image Processing*, vol. 14, no. 8, pp. 1138–1150, 2005.

[8] P. E. Debevec and J. Malik, "Recovering High Dynamic Range Radiance Maps from Photographs," in *Proceedings ACM SIGGRAPH*, 1997, pp. 369–378.

[9] A. A. Bell, C. Seiler, J. N. Kaftan, and T. Aach, "Noise in high dynamic range imaging," in *IEEE International Conference on Image Processing. ICIP 2008*, Oct. 2008, pp. 561–564.

[10] N. Barakat, A.N. Hone, and T.E. Darcie, "Minimal-bracketing sets for high-dynamic-range image capture," *IEEE Transactions on Image Processing*, vol. 17, no. 10, pp. 1864–1875, 2008.

[11] N. Barakat, T. E. Darcie, and A. N. Hone, "The tradeoff between SNR and exposure-set size in HDR imaging," in *IEEE International Conference on Image Processing. ICIP 2008*, Oct. 2008, pp. 1848–1851.

[12] C. Tomasi and R. Manduchi, "Bilateral filtering for gray and color images," in *International Conference on Computer Vision. ICCV 1998*, 1998, pp. 836–846.

[13] F. Catte, P.-L. Lions, J.-M. Morel, and T.Coll, "Image selective smoothing and edge-detection by nonlinear diffusion," *SIAM Journal on Numerical Analysis*, vol. 29, no. 1, pp. 182–193, 1992.

[14] David L. Donoho, "Nonlinear wavelet methods for recovery of signals, densities, and spectra from indirect and noisy data," in *In Proceedings of Symposia in Applied Mathematics*. 1993, pp. 173–205, American Mathematical Society.

[15] O. Tischenko, C. Hoeschen, and E.Buhr, "An artifact-free structure saving noise reduction using the correlation between two images for threshold determination in the wavelet domain," in *SPIE Medical Imaging*, 2005, pp. 1066–1075.

[16] A. Borsdorf, R. Raupach, T. Flohr, and J. Hornegger, "Wavelet Based Noise Reduction in CT-Images Using Correlation Analysis," *IEEE Transactions on Medical Imaging*, vol. 27, no. 12, pp. 1685–1703, 2008.

[17] M. W. Burke, *Image Acquisition. Handbook of Machine Vision Engineering. Volume 1*, Chapman and Hall, 1996.